Eur. Phys. J. C (2009) 64: 19–23
DOI 10.1140/epjc/s10052-009-1150-8

THE EUROPEAN
PHYSICAL JOURNAL C

Regular Article - Experimental Physics

Limits on a nucleon–nucleon monopole–dipole coupling from spin relaxation of polarized ultra-cold neutrons in traps

V.K. Ignatovich, Y.N. Pokotilovski[a]

Joint Institute for Nuclear Research, 141980 Dubna, Moscow Region, Russia

Received: 26 June 2009 / Published online: 19 September 2009

Abstract A new limit is presented on the axion-like monopole–dipole P, T-non-invariant interaction in a range (10^{-4}–1) cm. The spin-dependent nucleon–nucleon potential between neutrons and nucleons of the walls of the cavity containing ultra-cold neutrons should affect the neutron depolarization probability at their reflection from the walls. The limit is obtained from existing data on the ultra-cold neutron depolarization probability per one collision with the walls.

PACS 14.80.Mz · 12.20.Fv · 33.25.+k · 14.20.Dh

1 Introduction

Hypothetical pseudoscalar particle—axion offers a window to probe very small coupling and very high energy scales [1, 2].

Axion, according to later modifications of the primary model [1, 2], has mass in a very large range: ($10^{-12} < m_a < 10^6$) eV. Current algebra technique is used to relate the masses and coupling constants of the axion and neutral pion: $m_a = (f_\pi m_\pi/f_a)\sqrt{z}/(z+1)$, where $z = m_u/m_d = 0.56$, $f_\pi \approx 93$ MeV, $m_\pi = 135$ MeV, so that $m_a \approx (0.6 \times 10^{10}\ \text{GeV}/f_a)$ meV. Here f_a is the scale of Peccei–Quinn symmetry breaking. The axion coupling to fermions can be in general represented as $g_{\text{aff}} = C_f m_f/f_a$, where C_f is the model dependent factor [3, 4].

Early reactor, beam-dump, weak decays, and nuclear transition experiments have placed lower limits on the axion mass. Stringent limits, especially from the lower side of the axion mass range, have been set on the existence of axion using astrophysical and cosmological arguments [3, 5]. These more recent constraints limit the axion mass to ($10^{-5} < m_a < 10^{-3}$) eV with correspondingly very small coupling constants to quarks and photon [3–5]. Although these limits are more stringent than can be reached in laboratory experiments, it is of interest to try to constrain the axion as much as possible using laboratory means. Interpretation of laboratory experiments depend on less number of assumptions than the constraints inferred from astrophysical and cosmological observations and calculations. The laboratory experiments performed or proposed so far are rather diverse and employ a variety of detection techniques. Axion is still one of the candidates for the cold dark matter of the Universe [6, 7]. Some recent reviews are [3, 4].

2 Monopole–dipole interaction potential

Axions mediate a P- and T-odd monopole–dipole interaction potential between spin and matter (polarized and unpolarized nucleons) [8]:

$$U(\mathbf{r}) = (\boldsymbol{\sigma}\cdot\boldsymbol{n})\frac{g_s g_p \hbar^2}{8\pi m_n}\left(\frac{1}{\Lambda r}+\frac{1}{r^2}\right)e^{-r/\Lambda} = (\boldsymbol{\sigma}\cdot\boldsymbol{n})V_{ps}(r), \tag{1}$$

where g_s and g_p are dimensionless coupling constants of the scalar and pseudoscalar vertices (unpolarized and polarized particles), m_n is the nucleon mass at the polarized vertex, $\boldsymbol{\sigma}$ is vector of the Pauli matrices related to the nucleon spin, r is the distance between the nucleons, $\Lambda = \hbar/m_a c$ is the range of the force, m_a is the axion mass, and $\boldsymbol{n} = \boldsymbol{r}/r$ is the unit vector.

The microscopic potential (1) between two nucleons creates a macroscopic potential between nucleon and matter. If the matter is represented by a layer of thickness d, the neutron interaction with it is described by the potential

$$V(x) = (\boldsymbol{\sigma}\cdot\boldsymbol{n})g_s g_p\frac{\hbar^2 N\Lambda}{4m_n}e^{-x/\Lambda}\left(1-e^{-d/\Lambda}\right) = V_0(\boldsymbol{\sigma}\cdot\boldsymbol{n})e^{-x/\Lambda}\left(1-e^{-d/\Lambda}\right), \tag{2}$$

[a] e-mail: pokot@nf.jinr.ru

where x is the distance to the interface along the normal (unit vector $\boldsymbol{n}$), N is the nucleon density in the layer, and in the last equality we defined

$$V_0 = g_s g_p \frac{\hbar^2 N \Lambda}{4m_n}. \tag{3}$$

We will deal here only with ultra-cold neutrons (UCN) or total reflection of higher energy neutrons, and because of that we do not consider how the potential changes, when a neutron enters the matter.

Several laboratory searches provided constraints on axion-like coupling in the macroscopic range $\Lambda > 0.1$ cm [3, 9]. The limit in the Λ-range (10^{-4}–1) cm was established in the Stern–Gerlach type experiment in which UCN were transmitted through a slit between a horizontal mirror and absorber [10]. The obtained limit for the value $g_s g_p$ was $\sim 10^{-15}$ at $\Lambda = 10^{-2}$ cm, that corresponds to the value of the monopole–dipole interaction potential at the surface of the mirror $V_0 \sim 10^{-3}$ neV. This value is equivalent to an effective magnetic interaction $-\boldsymbol{\mu}\boldsymbol{B}$ of the neutron with magnetic field $B \sim 0.2$ G. It is estimated that in future ultra-cold neutron Stern–Gerlach type experiments sensitivity will be improved by orders of magnitude [11]. A better sensitivity is also expected in a proposed experiment on the ultra-cold neutron magnetic resonance frequency shift [12].

We consider here what limits on $g_s g_p$ in the range $\Lambda \div (10^{-4}$–1) cm can be extracted from depolarization of UCN in storage traps. Depolarization can be expected because the particle spin interaction with axion field $U_{\rm ax} = (\boldsymbol{\sigma}\cdot\boldsymbol{n})V$ is similar to magnetic interaction $U_{\rm magn} = |\mu|(\boldsymbol{\sigma}\cdot\boldsymbol{B})$ and corresponding pseudo-magnetic field in general is not collinear to the neutron polarization.

Depolarization was already considered earlier in the paper [13], however it was estimated there semiclassically as the neutron spin rotation in the interaction region Λ in vicinity of the reflecting wall, which is not sufficiently rigorous. Here we calculate the depolarization probability at a single collision with the wall with distorted wave Born approximation (DWBA) perturbation theory.

3 Constraints from the ultra-cold neutron depolarization

In fact, depolarization of UCN in traps can be attributed to many factors. In between them are inhomogeneities of the internal magnetic field and presence of magnetic impurities on the walls. We use here the most conservative estimate attributing all the neutron depolarization to the hypothetical axion-like interaction.

Let's consider a nonmagnetic semi-infinitely thick wall with optical potential u at $x > 0$, external homogeneous field $\boldsymbol{B}$ parallel to z-axis, and the axion pseudo magnetic field $b(x) = b_0 \exp(x/\Lambda)$ parallel to x-axis. We want to calculate spin-flip reflectivity of a neutron initial polarization along the $\boldsymbol{B}$ field, taking the axion field as a perturbation. For that we need to solve one dimensional stationary Schrödinger equation, which can be represented in the form

$$\begin{aligned}&\big[d^2/dx^2 + k^2 - B\sigma_z - b(x)\sigma_x \Theta(x<0)\\&\quad - u\Theta(x>0)\big]\big|\Psi(x)\big\rangle = 0,\end{aligned} \tag{4}$$

where $\sigma_{x,z}$ are the well known Pauli matrices, $\Theta(x)$ is a step function equal to unity, when inequality in its argument is satisfied, and to zero otherwise, k is normal component in vacuum of the wave vector of the incident particle, and the magnetic fields include factor $2m|\mu|/\hbar^2$, which contains neutron mass m and magnetic moment μ. To find a spinor solution $|\Psi(x)\rangle$ of (4) we need to define an incident wave $|\psi_0(x)\rangle$. In general we can define it as

$$\big|\psi_0(x)\big\rangle = \exp(i\hat{\boldsymbol{k}}x)|\xi\rangle, \tag{5}$$

where $\hat{\boldsymbol{k}} = \sqrt{k^2 - B\sigma_z}$, and $|\xi\rangle$ is an arbitrary spin state, which is a superposition $|\xi\rangle = \alpha|\xi_u\rangle + \beta|\xi_d\rangle$ of states $|\xi_{u,d}\rangle$ that are eigen spinors of the matrix σ_z: $\sigma_z|\xi_{u,d}\rangle = \pm|\xi_{u,d}\rangle$.

A non-perturbed solution of (4) is

$$\begin{aligned}\big|\Psi_0(x)\big\rangle = \big\{&\Theta(x<0)\big[e^{i\hat{\boldsymbol{k}}x} + e^{-i\hat{\boldsymbol{k}}x}\hat{\boldsymbol{r}}(k)\big]\\&+ \Theta(x>0)\hat{\boldsymbol{t}}(k)e^{i\hat{\boldsymbol{k}}'x}\big\}|\xi\rangle,\end{aligned} \tag{6}$$

where $\hat{\boldsymbol{k}}' = \sqrt{k^2 - B\sigma_z - u}$, reflection, $\hat{\boldsymbol{r}}$, and transmission, $\hat{\boldsymbol{t}}$, matrices determined (see, for instance [14]) from matching conditions at the interface are

$$\hat{\boldsymbol{r}}(k) = \frac{\hat{\boldsymbol{k}} - \hat{\boldsymbol{k}}'}{\hat{\boldsymbol{k}} + \hat{\boldsymbol{k}}'}, \qquad \hat{\boldsymbol{t}}(k) = \frac{2\hat{\boldsymbol{k}}}{\hat{\boldsymbol{k}} + \hat{\boldsymbol{k}}'}. \tag{7}$$

It is seen that the spinor (6) can be represented as $|\Psi_0(x)\rangle = \hat{\boldsymbol{\Psi}}_0(x)|\xi\rangle$, where $\hat{\boldsymbol{\Psi}}_0(x)$ is 2×2 matrix

$$\begin{aligned}\hat{\boldsymbol{\Psi}}_0(x) = {}&\Theta(x<0)\big[\exp(i\hat{\boldsymbol{k}}x) + \exp(-i\hat{\boldsymbol{k}}x)\hat{\boldsymbol{r}}(k)\big]\\&+ \Theta(x>0)\exp(i\hat{\boldsymbol{k}}'x)\hat{\boldsymbol{t}}(k).\end{aligned} \tag{8}$$

This matrix satisfies the non-perturbed Schrödinger equation

$$\big[d^2/dx^2 + k^2 - B\sigma_z - u\Theta(x>0)\big]\hat{\boldsymbol{\Psi}}_0(x) = 0, \tag{9}$$

and is diagonal one, which means that its non-diagonal matrix elements

$$\begin{aligned}\hat{\boldsymbol{\Psi}}_0(x)_{du} &= \langle\xi_d|\hat{\boldsymbol{\Psi}}_0(x)|\xi_u\rangle,\\ \hat{\boldsymbol{\Psi}}_0(x)_{ud} &= \langle\xi_u|\hat{\boldsymbol{\Psi}}_0(x)|\xi_d\rangle\end{aligned} \tag{10}$$

are zero.

The perturbation $b(x)\sigma_x$ changes (6), and the change $|\delta\Psi(x)\rangle = \delta\hat{\boldsymbol{\Psi}}(x)|\xi\rangle$, according to perturbation theory is representable as

$$\delta\hat{\boldsymbol{\Psi}}(x) = \int \hat{\boldsymbol{G}}(x,x')b(x')\sigma_x\hat{\boldsymbol{\Psi}}_0(x')\,dx', \tag{11}$$

where the matrix Green function, $\hat{\boldsymbol{G}}$, in the DWBA approach is a causal solution of the inhomogeneous Schrödinger equation:

$$\begin{aligned}&\big[d^2/dx^2 + k^2 - B\sigma_z - u\Theta(x>0)\big]\hat{\boldsymbol{G}}(x,x')\\&\quad = \hat{\boldsymbol{I}}\delta(x-x').\end{aligned} \tag{12}$$

Here $\hat{\boldsymbol{I}}$ in the right hand side is the unit matrix. Solution of this eqnarray is constructed with the help of two linearly independent solutions $\hat{\boldsymbol{\Psi}}_{1,2}(x)$ of (9):

$$\begin{aligned}\hat{\boldsymbol{G}}(x,x') = \hat{\boldsymbol{w}}^{-1}\big[&\Theta(x>x')\hat{\boldsymbol{\Psi}}_1(x)\hat{\boldsymbol{\Psi}}_2(x')\\&+\Theta(x<x')\hat{\boldsymbol{\Psi}}_2(x)\hat{\boldsymbol{\Psi}}_1(x')\big],\end{aligned} \tag{13}$$

where $\hat{\boldsymbol{w}}$ is their Wronskian

$$\hat{\boldsymbol{w}} = \big[\hat{\boldsymbol{\Psi}}_1'(x)\hat{\boldsymbol{\Psi}}_2(x) - \hat{\boldsymbol{\Psi}}_2'(x)\hat{\boldsymbol{\Psi}}_1(x)\big], \tag{14}$$

and prime means derivative over x: $\hat{\boldsymbol{\Psi}}'(x) = d\hat{\boldsymbol{\Psi}}(x)/dx$.

For $\hat{\boldsymbol{\Psi}}_1(x)$ we can take solution (8): $\hat{\boldsymbol{\Psi}}_1(x) = \hat{\boldsymbol{\Psi}}_0(x)$, and for linear independent solution $\hat{\boldsymbol{\Psi}}_2(x)$ we can take

$$\begin{aligned}\hat{\boldsymbol{\Psi}}_2(x) = {}&\Theta(x<0)\exp(-i\hat{\boldsymbol{k}}x)\hat{\boldsymbol{t}}'(k)\\&+\Theta(x>0)\big[\exp(-i\hat{\boldsymbol{k}}'x) + \exp(i\hat{\boldsymbol{k}}x)\hat{\boldsymbol{r}}'(k)\big],\end{aligned} \tag{15}$$

where matching conditions satisfy for

$$\begin{aligned}\hat{\boldsymbol{r}}'(k) &= \frac{\hat{\boldsymbol{k}}' - \hat{\boldsymbol{k}}}{\hat{\boldsymbol{k}} + \hat{\boldsymbol{k}}'} = -\hat{\boldsymbol{r}}(k),\\ \hat{\boldsymbol{t}}'(k) &= \frac{2\hat{\boldsymbol{k}}'}{\hat{\boldsymbol{k}} + \hat{\boldsymbol{k}}'}.\end{aligned} \tag{16}$$

The Wronskian of $\hat{\boldsymbol{\Psi}}_{1,2}(x)$ is equal to

$$\hat{\boldsymbol{w}} = 2i\hat{\boldsymbol{k}}\hat{\boldsymbol{t}}'(k). \tag{17}$$

Substitution of all these matrices into (11) gives $\delta\hat{\boldsymbol{\Psi}}(x) = \exp(-i\hat{\boldsymbol{k}}x)\hat{\boldsymbol{R}}$, where

$$\begin{aligned}\hat{\boldsymbol{R}} = \int_{-\infty}^{0}&\frac{dx'}{2i\hat{\boldsymbol{k}}}\big[e^{i\hat{\boldsymbol{k}}x'} + e^{-i\hat{\boldsymbol{k}}x'}\hat{\boldsymbol{r}}(k)\big]b(x')\\&\times\sigma_x\big[e^{i\hat{\boldsymbol{k}}x'} + e^{-i\hat{\boldsymbol{k}}x'}\hat{\boldsymbol{r}}(k)\big].\end{aligned} \tag{18}$$

The searched amplitude of spin flip reflection is

$$\hat{\boldsymbol{R}}_{du} = \langle\xi_d|\hat{\boldsymbol{R}}|\xi_u\rangle. \tag{19}$$

Substitution of (18) gives

$$\begin{aligned}\hat{\boldsymbol{R}}_{du} = \int_{-\infty}^{0}&\frac{dx'}{2ik_d}\big[e^{ik_dx'} + e^{-ik_dx'}r_d(k)\big]b(x')\\&\times\big[e^{ik_ux'} + e^{-ik_ux'}r_u(k)\big],\end{aligned} \tag{20}$$

where $k_{u,d} = \sqrt{k^2 \mp B}$,

$$\begin{aligned}r_{u,d}(k) &= \frac{k_{u,d} - k'_{u,d}}{k_{u,d} + k'_{u,d}},\\ k_{u,d} &= \sqrt{k^2 \mp B},\; k'_{u,d} = \sqrt{k^2 - u \mp B}.\end{aligned} \tag{21}$$

Substitution of $b(x) = b_0\exp(qx)$, where $q = 1/\Lambda$, and integration over x' in (20) gives

$$\begin{aligned}\hat{\boldsymbol{R}}_{du} &= \frac{b_0}{2ik_d}\bigg(\frac{1}{q+i(k_u+k_d)} + \frac{r_ur_d}{q-i(k_u+k_d)}\\&\quad+\frac{r_d}{q+i(k_u-k_d)} + \frac{r_u}{q-i(k_u-k_d)}\bigg)\\&= \frac{b_0}{2ik_d}\bigg(\frac{q(1+r_ur_d) - i(k_u+k_d)(1-r_ur_d)}{q^2+(k_u+k_d)^2}\\&\quad+\frac{q(r_d+r_u) - i(k_u-k_d)(r_d-r_u)}{q^2+(k_u-k_d)^2}\bigg).\end{aligned} \tag{22}$$

In the case of total reflection and not large external field ($U_{\text{magn}} = |\mu|(\boldsymbol{\sigma}\cdot\boldsymbol{B}) \ll E_n$) we can approximate $k_u + k_d \approx 2k$, $k_u - k_d \approx -B/k$ and $r_u \approx r_d = \exp(-2i\phi)$, where $\phi = \arccos(k/\sqrt{u})$. In this approximation the (22) is reduced to

$$\begin{aligned}\hat{\boldsymbol{R}}_{du} = e^{-2i\phi}\frac{b_0}{ik}\bigg(&\frac{q\cos(2\phi) + 2k\sin(2\phi)}{q^2+4k^2}\\&+\frac{q}{q^2+B^2/k^2}\bigg).\end{aligned} \tag{23}$$

As we are interested in the interaction range satisfying to $k\Lambda \gg 1$ (typical UCN $k \sim 10^6\ \text{cm}^{-1}$, $\Lambda > 10^{-4}$ cm) and not too strong external magnetic fields (<~500 G), the first term in (23) can be neglected comparing to the second one:

$$\hat{\boldsymbol{R}}_{du} = e^{-2i\phi}\frac{b_0}{ik}\bigg(\frac{q}{q^2+B^2/k^2}\bigg), \tag{24}$$

and the spin-flip reflectivity from the wall, represented in dimensional units, becomes

$$w = |\hat{\boldsymbol{R}}_{du}|^2 = \frac{4V_0^2\langle v_\perp\rangle^2(1-e^{-d/\Lambda})^2}{\Lambda^2\hbar^2(\frac{\langle v_\perp\rangle^2}{\Lambda^2} + \omega_0^2)^2}, \tag{25}$$

where $\omega_0 = \gamma_n B$ is the neutron spin Larmor frequency in the external field B, $\gamma_n = 1.83\times10^4\ \text{s}^{-1}$/G—the gyromagnetic ratio for the neutron, $\langle v_\perp\rangle$ is the averaged over the UCN spectrum normal to the surface neutron velocity component.

At $\omega_0 \gg \langle v_\perp \rangle/\Lambda$ we have the expression coinciding with the one obtained for the quasiclassical case and derived in the [15] with ω_0^{-4} behavior of the depolarization probability. Typically $\langle v_\perp \rangle \sim 300$ cm/s, and for $\Lambda = 10^{-4}$ cm the quasiclassical case is valid at $B > 100$ G.

At a weak guiding magnetic field $\sim 10^{-2}$ G the quasiclassical approach is valid only for the interaction range $\Lambda > \langle v_\perp \rangle/\omega_0 \sim 1$ cm.

Substituting (2) into (25) we obtain the expression for $g_s g_p$:

$$g_s g_p \simeq \beta^{1/2} \frac{2 m_n}{\hbar N \langle v_\perp \rangle (1 - e^{-d/\lambda})} \times \left(\frac{\langle v_\perp \rangle^2}{\lambda^2} + \omega_0^2 \right), \qquad (26)$$

where β is the experimentally measured UCN depolarization probability per one reflection from the wall of the storage cavity.

There are two published experimental data on the ultra-cold neutron depolarization: [16, 17] and [18], in which special experiments are described to measure this value. In both publications, for a variety of materials, the measured values of the neutron depolarization probability per one neutron collision with the walls of storage cavity were around $\beta \sim 10^{-5}$. The $\beta \sim 10^{-6}$ was measured in [18] for the diamond like carbon foils (DLC). The magnetic fields in the storage chambers were partly due to stray fields from strong magnets used for the polarization of the incident neutrons [16–18] and partly were formed by special magnets [18]. In [16, 17] magnetic field was estimated [19] to be near 50 G, and in the experiment [18] it was reported to be ~ 55 G. In both cases, this rather large external magnetic field suppressed effect of the additional hypothetical spin-dependent interaction on depolarization of the ultra-cold neutrons in traps, and therefore decreased sensitivity of these measurements to establishing constraints on the axion-like interaction.

A better constraints can be obtained from the measurements of the ultra-cold neutron depolarization in traps at lower magnetic field B_z in the experiments on the search for the neutron electric dipole moment (EDM) [20] and [21–23]. There the ultra-cold neutrons preliminary polarized by transmission through magnetized ferromagnetic foil were stored in a cylindrical bottle permeated by magnetic and electric fields. The magnetic field was applied parallel to the axis of the bottle, and its value in these experiments was very low: $B_z = 0.02$ G in [20], and $B_z = 0.01$ G in [21–23]. The change of the magnetic resonance frequency was sought for at the reverse of the electric field direction. After filling the bottle with ultra-cold neutrons and closing the neutron valve, the $\pi/2$ Ramsey pulse was applied, which turned neutron spins perpendicular to the magnetic field. The neutrons were allowed to precess about magnetic field for 130 s [21–23], after which the second $\pi/2$ Ramsey pulse was applied, and neutrons in the appropriate spin state passed back through the polarizing foil to the neutron detector.

Depolarization of neutrons at reflections from the walls of the storage cavity in presence of a gradient of a spin-dependent potential decreases contrast of the neutron magnetic resonance curves. Probability of the neutron depolarization was not measured directly in these experiments, but from the reported very good magnetic resonance curves it can be concluded that the UCN depolarization probability at a single collision with the walls was not higher than in [16–18]. According to [24] the neutron depolarization time in the EDM experiment [21–23] can be estimated to be not less than $\tau_{\text{dep}} \sim 800$ s. From this figure we can estimate the depolarization probability per single collision with the walls: $\beta = l/(\tau_{\text{dep}} v) = 18/(800 \times 500) \sim 4 \times 10^{-5}$, where l is the mean free path between two consecutive collisions, which can be found from dimensions of the neutron bottle: in the experiment [21–23] it was a cylinder of the internal diameter about 44 cm and height 15 cm. We constrain the monopole–dipole interaction in two assumptions for the depolarization probability in [21–23]: one—$\beta = 4 \times 10^{-5}$, and another one—corresponding to the best value obtained in the experiments of the PSI group [18]—$\beta = 10^{-6}$.

With above β we can draw the limiting curves for the parameters of the monopole–dipole coupling of the axion field, which is shown in Fig. 1 together with results from other publications.

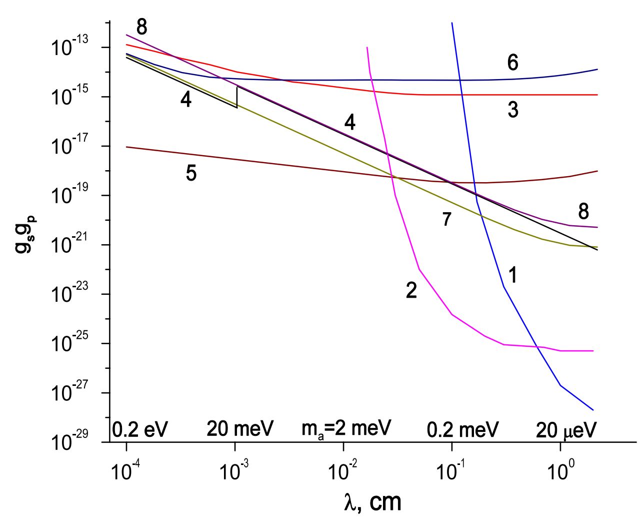

Fig. 1 Constraints on the axion monopole-dipole coupling strength $g_s g_p$ and effective range: *1* and *2*—constraints for the value of coupling constant of nucleon and electron $g_s g_p^e$ from [25, 26] and [9], respectively; *3*—from the neutron gravity experiment of [10], *4*—from [13], *5*—from spin relaxation of ^{3}He, [27], *6*—this work at the UCN depolarization probability $\beta = 10^{-6}$ and magnetic field $B_z = 50$ G [18], *7*—the same, but $B_z = 0.01$ G [21–23]; *8*—the same, but $B_z = 0.01$ G, $\beta = 4 \times 10^{-5}$ [21–24]. It was assumed in both cases of the ultra-cold neutron storage, that $d = 1$ cm, $N \approx 2 \times 10^{24}$ cm^{-3}, $\langle v_\perp \rangle = 300$ cm/s

The ultra-cold neutron depolarization data may be used also to set limits on the monopole–dipole coupling between neutrons and electrons of the walls of the storage chambers. However, because density of the electrons in the medium is approximately two times lower than the density of nucleons, the constraints are respectively two times less strong.

References

1. S. Weinberg, Phys. Rev. Lett. **40**, 223 (1978)
2. F. Wilczek, Phys. Rev. Lett. **40**, 279 (1978)
3. C. Hangmann, H. Murayama, G.G. Raffelt et al. (Particle Data Group), Phys. Lett. B **667**, 459 (2008)
4. L.J. Rosenberg, K.A. van Bibber, Phys. Rep. **325**, 1 (2000)
5. M.S. Turner, Phys. Rep. **197**, 67 (1990)
6. P. Sikivie, Phys. Rev. Lett. **51**, 1415 (1983)
7. R. Bradley, J. Clarke, D. Kinion et al., Rev. Mod. Phys. **75**, 777 (2003)
8. J.E. Moody, F. Wilczek, Phys. Rev. D **30**, 130 (1984)
9. G.D. Hammond, C.C. Speake, Ch. Trenkel, A. Pulido-Patón, Phys. Rev. Lett. **98**, 081101 (2007)
10. S. Baeßler, V.V. Nesvizhevsky, K.V. Protasov et al., Phys. Rev. D **75**, 075006 (2007)
11. S. Baeßler, V.V. Nesvizhevsky, G. Pignol et al., arXiv:0902.3139v1 [nucl-ex]
12. O. Zimmer, arXiv:0810.3215v1 [nucl-ex]
13. A.P. Serebrov, arXiv:0902.1056 [nucl-ex]
14. F. Radu, V.K. Ignatovich, Generalized matrix method for the transmission of neutron through multilayer magnetic system with noncollinear magnetization. Physica B **267–268**, 175–180 (1999)
15. Yu.N. Pokotilovski, Pis'ma Zh. Eksp. Teor. Fiz. **76**, 162 (2002); [JETP Lett. **76**, 131 (2002); Erratum in JETP Lett. **78**, 422 (2002)]
16. A.P. Serebrov, M.S. Lasakov, A. Vasilijev et al., Nucl. Instrum. Methods A **440**, 715 (2000)
17. A.P. Serebrov, M.S. Lasakov, A. Vasilijev et al., Phys. Lett. A **313**, 373 (2003)
18. F. Atchison, B. Brys, M. Daum et al., Phys. Rev. C **76**, 044001 (2007)
19. A.P. Serebrov, Private communication
20. I.S. Altarev, Yu.V. Borisov, N.V. Borovikova et al., Yad. Fiz. **59**, 1204 (1996); [Phys. At. Nucl. **59**, 1152 (1996)]
21. K.F. Smith, N. Crampin, J.M. Pendlebury et al., Phys. Lett. B **234**, 191 (1990)
22. F.G. Harris, C.A. Baker, K. Green et al., Phys. Rev. Lett. **82**, 904 (1999)
23. C.A. Baker, D.D. Doyle, P. Geltenbort et al., Phys. Rev. Lett. **97**, 131801 (2006)
24. S. Ivanov, Private communication
25. R.C. Ritter, L.I. Winkler, G.T. Gillies, Phys. Rev. Lett. **70**, 701 (1993)
26. W.-T. Ni, S.-S. Pan, S.-C. Yeh et al., Phys. Rev. Lett. **82**, 2439 (1999)
27. Yu.N. Pokotilovski, arXiv:0902.1682 [nucl-ex]